[CANCER RESEARCH 64, 689–695, January 15, 2004]

Selective Growth Inhibition of Tumor Cells by a Novel Histone Deacetylase Inhibitor, NVP-LAQ824

Peter Atadja, Lin Gao, Paul Kwon, Nancy Trogani, Heather Walker, Meier Hsu, Lakshmi Yeleswarapu, Nagarajan Chandramouli, Larry Perez, Richard Versace, Arthur Wu, Lidia Sambucetti, Peter Lassota, Dalia Cohen, Kenneth Bair, Alexander Wood, and Stacy Remiszewski

Department of Oncology, Novartis Institutes for Biomedical Research, East Hanover, New Jersey

ABSTRACT

We have synthesized a histone deacetylase inhibitor, NVP-LAQ824, a cinnamic hydroxamic acid, that inhibited *in vitro* enzymatic activities and transcriptionally activated the p21 promoter in reporter gene assays. NVP-LAQ824 selectively inhibited growth of cancer cell lines at submicromolar levels after 48–72 h of exposure, whereas higher concentrations and longer exposure times were required to retard the growth of normal dermal human fibroblasts. Flow cytometry studies revealed that both tumor and normal cells arrested in the G_2-M phase of the cell cycle after compound treatment. However, an increased sub-G_1 population at 48 h (reminiscent of apoptotic cells) was observed only in the cancer cell line. Annexin V staining data supported our hypothesis that NVP-LAQ824 induced apoptosis in tumor and transformed cells but not in normal cells. Western blotting experiments showed an increased histone H3 and H4 acetylation level in NVP-LAQ824-treated cancer cells, suggesting that the likely *in vivo* target of NVP-LAQ824 was histone deacetylase(s). Finally, NVP-LAQ824 exhibited antitumor effects in a xenograft animal model. Together, our data indicated that the activity of NVP-LAQ824 was consistent with its intended mechanism of action. This novel histone deacetylase inhibitor is currently in clinical trials as an anticancer agent.

INTRODUCTION

Coordinated and precise regulation of gene expression is critical for maintenance of normal cell growth and differentiation (reviewed in Ref. 1). In eukaryotic cells, DNA is packaged into chromatin, and to alter gene expression, a dynamic process is required: local remodeling of nucleosomes (1). Reversible acetylation is one such process facilitated by histone acetyltransferases and histone deacetylases (HDACs). Transcriptionally active chromatin regions, such as the euchromatin, are associated with hyperacetylated histones, whereas transcriptionally silent heterochromatin regions are generally hypoacetylated (reviewed in Ref. 1). Both histone acetyltransferases and HDACs are recruited to target genes in complexes with sequence-specific factors and cofactors to regulate gene expression and ultimately cell function.

Inappropriate expression of genes required for cell proliferation, differentiation, or tumor suppression has been linked to cancer. Several lines of evidence suggest that aberrant recruitment of HDACs and the resulting chromatin modifications may lead to changes in gene expression seen in transformed cells: (*a*) silencing of tumor suppressor genes at the chromatin level (2–8); (*b*) interaction of HDAC-containing complexes with proteins involved in tumorigenesis (9–11); (*c*) reports of HDAC inhibitors (HDACIs) having significant antiproliferative effects, such as promoting differentiation, cell cycle arrest, or apoptosis (12–17); and (*d*) induction of key mediators of G_1 cell cycle arrest and differentiation, such as p21 with HDACIs (12, 18–21). Studies of hematological malignancies also support involvement of HDACs in cancer development and/or maintenance. Aberrant recruitment of HDAC complexes is necessary for the carcinogenic properties of the fusion proteins PLZF-RARα, PML-RARα, and AML1/ETO in acute leukemia (reviewed in Ref. 22). In t(8;21) acute myelocytic leukemia (AML), HDAC-mediated repression of target genes such as *AML1* blocked differentiation of hematopoietic precursors (23, 24). In acute promyelocytic leukemia with t(11;17)/*PLZF-RAR*α translocation, a combination of all-*trans* retinoic acid with the HDACI trichostatin resulted in differentiation of all-*trans* retinoic acid-resistant acute promyelocytic leukemia cells (25). Furthermore, treatment of leukemic blasts obtained from non-acute promyelocytic leukemia AML patients with a combination of retinoic acid and trichostatin induced terminal myeloid differentiation (26).

Preclinical experiments using small molecule inhibitors of HDACs, such as MS-275 and suberoylanilide hydroxamic acid (SAHA), exhibited efficacy against several human tumor xenografts in athymic mice (19, 27). In addition, the natural product HDACIs of the trapoxin class and trichostatin were shown to activate the p21 promoter, increase p21 protein levels, inhibit cyclin-dependent kinase 2 kinase activity, reduce retinoblastoma (Rb) phosphorylation, and cause cell cycle arrest or apoptosis in three human tumor cell lines (21, 28, 29). NVP-LAQ824, our novel synthetic HDACI, showed similar properties at submicromolar concentrations. Our studies also indicated that NVP-LAQ824 induced apoptosis in tumor cells but cell cycle arrest in normal fibroblasts. Moreover, increased histone acetylation in NVP-LAQ824-treated cancer cells confirmed the activity of our compound against HDACs. We therefore conclude that the antitumor effect seen was, in fact, attributable to specific inhibition of HDAC.

MATERIALS AND METHODS

Materials. NVP-LAQ824 was prepared in-house as the lactate salt and dissolved in DMSO. MS-275 was prepared as described in Suzuki *et al.* (29) as a free base and was dissolved in DMSO. Suberoylanilide hydroxamic acid (SAHA) was prepared as described in Richon *et al.* (30) and was dissolved in DMSO. The ECF Western blotting reagent pack for mouse or rabbit was purchased from Amersham Pharmacia Biotech Inc. (Piscataway, NJ). Pre-cast NuPAGE gels were from Invitrogen Life Technologies, Inc. (Carlsbad, CA). The CellTiter 96 AQueous Non-Radioactive Cell Proliferation Assay was from Promega (Madison, WI). The ApoAlert Annexin V Apoptosis kit was from Clontech Laboratories, Inc. (Palo Alto, CA). The Hybond-P, polyvinylidene difluoride, membrane was purchased from Amersham Biosciences (Piscataway, NJ).

Cell Culture. H1299, HCT116, A549, DU145, PC3, and MDA435 cells were obtained from American Type Culture Collection (Rockville, MD) and were maintained according to the supplier's instructions. Normal dermal human fibroblast (NDHF) and normal human bronchial epithelial (NHBE) cells were obtained from Clonetics (San Diego, CA) and were maintained in DMEM supplemented with 15% fetal bovine serum, 100 units/ml penicillin, 100 μg/ml streptomycin, and BEGM BulletKit (Clonetics, San Diego, CA) supplemented with retinoic acid. hTERT/SV40 T antigen-transformed NHBE (hTERT/SV40 NHBE) cells were a kind gift from Dr. Barrett Rollins (Dana-Farber Cancer Institute, Harvard Medical Center, Boston, MA) and were maintained in BEGF BulletKit supplemented with retinoic acid.

Received 7/9/03; revised 11/7/03; accepted 11/10/03.

The costs of publication of this article were defrayed in part by the payment of page charges. This article must therefore be hereby marked *advertisement* in accordance with 18 U.S.C. Section 1734 solely to indicate this fact.

Requests for reprints: Peter Atadja, Oncology Molecular and Cellular Biology Unit, Novartis Institutes for Biomedical Research, East Hanover, NJ 07936. Phone: (862) 778-0435; Fax: (973) 781-7578; E-mail: peter.atadja@pharma.novartis.com.

Enzyme Purification and *in Vitro* Histone Deacetylase Assay. HDAC enzymes were partially purified from H1299 cell lysate by ion exchange chromatography using the Q Sepharose Fast Flow column (Amersham Biosciences). The assay was performed as described previously (20) using the partially purified cell lysate and ^{3}H-labeled acetylated histone-H4 peptide as the substrate. All enzymatic assays were performed in triplicate and indicated as the mean ± SD.

p21 Promoter Activation Assay. The plasmid encoding the luciferase gene driven by the p21 promoter and its transfection into H1299 cells were described previously (20). Data were analyzed by calculating mean fold activation ($n = 3$) of compound-treated cells compared with the average of DMSO-treated control ($n = 3$). The percentage of activity for each concentration of NVP-LAQ824 was determined by comparison with the maximal fold activation obtained from psammaplin A, a natural product identified from a screen for p21 promoter activation (32).[1] The AC_{50}s were calculated using a linear regression calculation between data points to predict the concentration of compound needed for 50% activation relative to the reference.

Monolayer Growth Inhibition Assay. Cell proliferation was measured using an adaptation of published procedures (3-(4,5-dimethylthiazol-2-yl)-5-(3-carboxymethoxy-phenyl)-2-(4-sulfonyl)-2*H*-tetrazolium assay) as described previously (29). The CellTiter 96 AQueous Non-Radioactive Cell Proliferation Assay was performed according to the manufacturer's protocol. The average background value (treatment with medium alone) was subtracted from each experimental well; triplicate values were averaged for each compound dilution. The following formulas were used to calculate the percentage of growth:

$$If\ X > T_0, \%\ \text{Growth} = ((X - T_0)/(GC - T_0)) \times 100$$

$$If\ X < T_0, \%\ \text{Growth} = (X - T_0)/T_0 \times 100$$

where T_0 is the average value of T_0 − background, GC is the average value of untreated cells (in triplicate) − background, and X is the average value of compound-treated cells (in triplicate) − background.

The "% Growth" was plotted against compound concentration and used to calculate the IC_{50} using the linear regression techniques between data points to predict the concentration of compounds at 50% inhibition.

Cell Cycle Analysis. HCT116 and NDHF cells (1×10^6 each) were seeded on 10-cm^2 tissue culture dishes and were allowed to grow overnight at 37°C with 5% CO_2. HCT116 and NDHF cells were exposed to 0.1 and 0.5 μM NVP-LAQ824, respectively, or 0.1% DMSO. In addition, HCT116 cells were treated with 1 μM SAHA and 10 μM MS-275. After 24 and 48 h, the cells were collected, briefly resuspended in ice-cold 70% ethanol, and incubated in propidium iodide solution (70 μM propidium iodide, 38 mM sodium citrate, and 20 μg/ml RNase A) at 37°C for 30 min. Flow cytometric analysis was performed on a FACSort instrument (Becton Dickinson Immunocytometry Systems, San Jose, CA), and the data were subsequently analyzed using the ModFit^{LT} software (Becton Dickinson).

Apoptosis Detection. A549, HCT116, and NDHF cells (3×10^5 each) as well as NHBE and human telomerase reverse transcriptase (hTERT)/SV40 NHBE cells (1.5×10^5 each) were seeded in a 24-well plate (Costar Inc., Corning, NY). Twenty-four h later, cells were incubated with NVP-LAQ824 at the indicated concentrations or 0.1% DMSO as the control. Twenty-four and/or 48 h after NVP-LAQ824 treatment, the medium was removed, and the cells were incubated in the dark for 15 min with binding buffer containing 1 μg/ml Annexin V-FITC and 2.5 μg/ml propidium iodide. The cells were observed with a fluorescent microscope using a dual filter set for FITC and rhodamine.

Western Blot Analysis. HCT116 and A549 tumor cells (1×10^6 each) were treated with the indicated concentrations of NVP-LAQ824 for the appropriate times. The treated cells were lysed in 500 μl of ice-cold triple detergent buffer [50 mM Tris-Cl (pH 8.0), 150 mM NaCl, 0.02% sodium azide, 0.1% SDS, 1% NP40, 0.5% sodium deoxycholate, and 10 μl/ml protease inhibitor mixture). Cell lysates (10 μg) were separated on a 4–12% NuPAGE gel by electrophoresis and transferred onto the Hybond-P, polyvinylidene difluoride, membrane. The membranes were probed with anti-p21^{waf1} antibody (Oncogene Research Products, San Diego, CA) diluted 1:100, anti-Rb antibody (PharMingen, San Diego, CA) diluted 1:1000, anti-acetylated H3 antibody (Upstate Technologies, Lake Placid, NY) diluted 1:1000, anti-acetylated H4 antibody (Upstate Technologies, Lake Placid, NY) diluted 1:250, and anti-glyceraldehyde-3-phosphate dehydrogenase (GAPDH) antibody (Chemicon Inernational Inc., Temecula, CA) diluted 1:1000 for 2 h at room temperature or overnight at 4°C. The specific protein signals were detected using the ECF Western blotting reagent pack and the Storm 860 Phosphorimager (Molecular Dynamics, Sunnyvale, CA) after appropriate secondary antibody incubation.

Tumor Xenografts Implantation. The studies were performed on-site, using outbred athymic (*nu/nu*) female mice (Hsd:Athymic Nude-nu from Harlan Sprague Dawley, Indianapolis, IN). Mice were anesthetized with Metofane (Mallinckrodt Veterinary, Inc., Mundelein, IL), and a cell suspension (100 μl) containing 1×10^6 HCT116 cells was injected s.c. into the right axillary (lateral) region of each animal. Tumors were allowed to reach the volume of approximately 100–400 mm^3. At this point, mice bearing tumors with acceptable morphology (non-necrotic) and of similar size range were selected and distributed into groups of six for the studies. NVP-LAQ824 was dissolved in DMSO to create a stock solution, which was further diluted just before dosing with D5W to a final DMSO concentration of 10%. Tumor-bearing mice were treated with the compound by i.v. injection into the tail vein. NVP-LAQ824 was dosed once daily, 5 days/week, for a total of 15 doses. 5-Fluorouracil was administered at 100 mg/kg in 0.9% saline 1 day/week for a total of three doses. The control groups were treated with the vehicle. Tumors were collected from the animals at the indicated time points.

Statistical Analysis. All *in vitro* experiments were conducted in triplicate and repeated at least three times. The results are presented as mean activity values, IC_{50} or AC_{50}, ± SD of the mean. Animal experiments were analyzed using the Student's t test for independence and were performed using the Sigmaplot software. $P < 0.05$ was determined to be significant.

RESULTS

NVP-LAQ824 Is a Potent HDACI *in Vitro*. We have designed and synthesized a novel HDACI, which we termed NVP-LAQ824 (33). NVP-LAQ824 is a cinnamic acid (structure shown in Fig. 1) that belongs to the hydroxamic acid-based group of HDACIs that includes trichostatin A, SAHA, and pyroxamide. Currently, several of these inhibitors are in clinical trials as cancer therapeutics (34–38).

The effect of NVP-LAQ824 on human HDAC activity was determined by *in vitro* HDAC enzyme assays. The 50% inhibitory concentration for NVP-LAQ824 was remarkably similar over several independent experiments and was determined to be at a low nanomolar concentration (Table 1). Thus, NVP-LAQ824 is a potent inhibitor of HDAC activity.

NVP-LAQ824 Activated the p21 Promoter and Inhibited Cell Proliferation. Inhibitors of HDACs activate the expression of the gene encoding the p21 cell cycle inhibitor (18–20, 39). To determine the effect of NVP-LAQ824 on *p21* gene expression, transcriptional activation of a transiently transfected p21 promoter driving a luciferase reporter gene was measured in H1299 cells. The concentration of NVP-LAQ824 producing 50% of the maximal promoter activation (AC_{50}) relative to psammaplin A, a natural product identified in a screen for inducing the p21 promoter, was shown in Table 1. These results demonstrated that nanomolar concentrations of NVP-LAQ824 were needed to induce the reporter construct, indicating specificity of the compound for the p21 promoter.

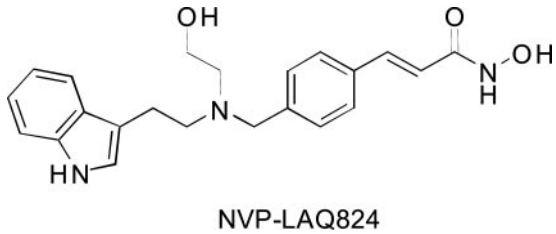

NVP-LAQ824

Fig. 1. Chemical structure of NVP-LAQ824.

[1] Perez, L. B., Atadja, P., Bair, K., Cornell, W., Dean, K., Green, M., Kwon, P., Lamberson, C., Remisewski, S., Sambucetti, L., and Trogani, N. Exploring the structure-activity relationships of psammaplins: a new class of histone deacetylase inhibitors, manuscript in preparation.

Table 1 *In vitro activity profile of NVP-LAQ824*

The in vitro enzyme inhibition, p21 promoter activation, and growth inhibition assays were performed with various concentrations of NVP-LAQ824 and MS-275. HDAC enzyme assays and IC_{50}s from those assays were determined as described in "Materials and Methods." The p21 promoter activation assays were done in triplicate, as described in "Materials and Methods," and AC_{50} values are indicated. Inhibition of cell growth in monolayer after 72-h compound treatment was measured in triplicate by 3-(4,5-dimethylthiazol-2-yl)-5-(3-carboxymethyl-phenyl)-2-(4-sulfonyl)-2H-tetrazolium assays as described in "Materials and Methods." All experiments were repeated at least three times, and the indicated values represent the mean of IC_{50} or AC_{50} ± SD.

					Monolayer growth			
	HDAC enzyme		p21 promoter activation		H1299		HCT116	
Compound	IC_{50} (μM)	SD	AC_{50} (μM)	SD	IC_{50} (μM)	SD	IC_{50} (μM)	SD
NVP-LAQ824	0.032	0.018	0.30	0.20	0.15	0.015	0.010	0.002
MS-275	>10	NA[a]	7.8	0.9	6.8	1.1	0.67	0.12

[a] NA, not applicable.

Previous studies have demonstrated that HDACIs induce tumor cell growth arrest; therefore, we examined the effects of NVP-LAQ824 on the growth of tumor cell lines. Monolayer growth inhibition assays were performed (Tables 1 and 2). Results of these experiments revealed that continuous exposure to NVP-LAQ824 for 72 h inhibited the growth of both H1299, a non-small cell lung carcinoma line, and HCT116, a colon cancer cell line. The calculated IC_{50}s were 0.15 and 0.01 μM in H1299 and HCT116 cells, respectively. In contrast, the IC_{50}s for another HDACI, MS-275, were much higher. In addition, we examined the effects of NVP-LAQ824 in two prostate cancer cell lines (DU145 and PC3) and a breast cancer line (MDA435). The IC_{50}s in those cells were also in the nanomolar range (Table 2). Thus, low nanomolar concentrations of NVP-LAQ824 were sufficient to significantly inhibit growth of many tumor cells.

The Antiproliferative Effect of NVP-LAQ824 Is Selective to Human Tumor Cells. For the potential use of NVP-LAQ824 as an anticancer agent, it must exhibit specificity for tumor cells at therapeutic doses (19). To determine whether NVP-LAQ824 is selective for cancer cells, NDHFs, colon carcinoma (HCT116), and non-small cell lung carcinoma (A549) cells were exposed to various concentrations of NVP-LAQ824, and cell viability was measured at different time points (Table 3). In addition, antiproliferative effects of NVP-LAQ824 were measured with respect to duration of treatment. All three cell lines were exposed to NVP-LAQ824 for 3, 6, 16, 24, 48, and 72 h before the compound was washed out, and net cell growth was measured after 72 h (Fig. 2). For both experiments, LD_{50} and LD_{90} values were measured and defined as the concentrations of compound that caused 50 and 90% cell death, respectively. The results of these experiments showed that continuous exposure of NVP-LAQ824 for 72 h produced LD_{90}s of 0.09 μM in HCT116 cells and 0.47 μM in A549 cells (Table 3). Moreover, continuous treatment for up to 16 h, followed by incubation in drug-free medium, resulted in reduced net cell growth but not cell death. However, lethal effects were observed in HCT116 (Fig. 2*A*) and A549 (Fig. 2*B*) cells after 24 h of compound treatment. Interestingly, the LD_{90} was not achieved in either experiment with NDHFs, even at micromolar concentrations of NVP-LAQ824 tested (Table 3; Fig. 2*C*). Generally, HCT116 cells were more sensitive than A549 cells, with NDHFs having the least sensitivity to the growth-inhibitory effects of NVP-LAQ824 (Fig. 2*D*). These results indicated that the lethal effect of NVP-LAQ824 was time-dependent and exhibited a selective toxicity toward the tumor cell lines while inducing only growth arrest in normal fibroblasts.

Table 2 *Growth inhibitory effects of NVP-LAQ824 in several cancer cell lines*

Tumor cells, as indicated, were grown in monolayers and treated with NVP-LAQ824 at various concentrations. IC_{50}s were determined by 3-(4,5-dimethylthiazol-2-yl)-5-(3-carboxymethyl-phenyl)-2-(4-sulfonyl)-2H-tetrazolium assays and performed in replicates of three. The numbers represent the mean IC_{50}s ± SD.

	Cancer cell lines				
	H1299	HCT116	DU145	PC3	MDA435
NVP-LAQ824 IC_{50} (μM)	0.15	0.010	0.018	0.023	0.039

Table 3 *Time-dependent effects of NVP-LAQ824 on cell viability*

HCT116, A549, and NDHF cells were treated with various concentrations of NVP-LAQ824 for the indicated amount of time before the removal of the compound and the addition of fresh medium. Cell viability was measured at 72 h by 3-(4,5-dimethylthiazol-2-yl)-5-(3-carboxymethyl-phenyl)-2-(4-sulfonyl)-2H-tetrazolium assays as described in Table 1. Definitions of IC_{50}, LD_{50}, and LD_{90} were described in "Materials and Methods" and are indicated as the mean ± SD.

	IC_{50} (μM)	LD_{50} (μM)	LD_{90} (μM)
HCT116			
24 h	0.01	0.64	2.26
48 h	0.01	0.04	0.14
72 h	0.01	0.04	0.09
A549			
24 h	0.05	>3.75	>3.75
48 h	0.03	0.20	0.95
72 h	0.03	0.16	0.47
NDHF			
24 h	>3.75	>3.75	>3.75
48 h	0.13	>3.75	>3.75
72 h	0.04	0.61	>3.75

Lack of G_1-S Arrest in Tumor Cells Despite Induction of p21 Expression and Rb Hypophosphorylation by NVP-LAQ824. Increased expression of p21 results in inhibition of cyclin-dependent kinase activity and consequent hypophosphorylation of cyclin/cyclin-dependent kinase substrates such as Rb. Hypophosphorylation of Rb is associated with cell cycle arrest at G_1-S phase (12, 20). Consistent with previous findings, we observed a dose-dependent increase of p21 protein in A549 cells in response to NVP-LAQ824 treatment. Concomitant to the increased p21 level, we detected an increase in the hypophosphorylated state of the Rb tumor suppressor (Fig. 3). Thus, similar to many other HDACIs, NVP-LAQ824 was able to alter the expression level and change posttranslational modifications of key cell cycle regulators.

In light of the above findings as well as the observation that NVP-LAQ824 produced growth inhibition in cancer cell lines, we compared the cell cycle profiles of a normal cell line NDHF and a tumor cell line HCT116 subsequent to compound treatments. DMSO-treated cells were used as the negative control. NVP-LAQ824 treatment of NDHF cells caused the expected G_1-S growth arrest in addition to a significant reduction of cells in S-phase and accumulation of cells at the G_2-M checkpoint. These observations persisted through the 48-h treatment period without significant increases in sub-G_1 population (Fig. 4*A*). Exposure of HCT116 cells to HDACI revealed a surprising result. Treatment of HCT116 cells for 24 h with two other HDACIs, SAHA and MS-275, exhibited results consistent with the NDHF cells: G_1-S arrest, decreased S-phase, and G_2-M block. However, 24-h exposure of HCT116 cells to NVP-LAQ824 displayed no arrest at the G_1-S boundary despite experimental observations of p21 induction and Rb hypophosphorylation in tumor cells (Fig. 4*B*). These cells, nonetheless, maintained a significant decrease of S-phase and G_2-M cell cycle arrest. Moreover,

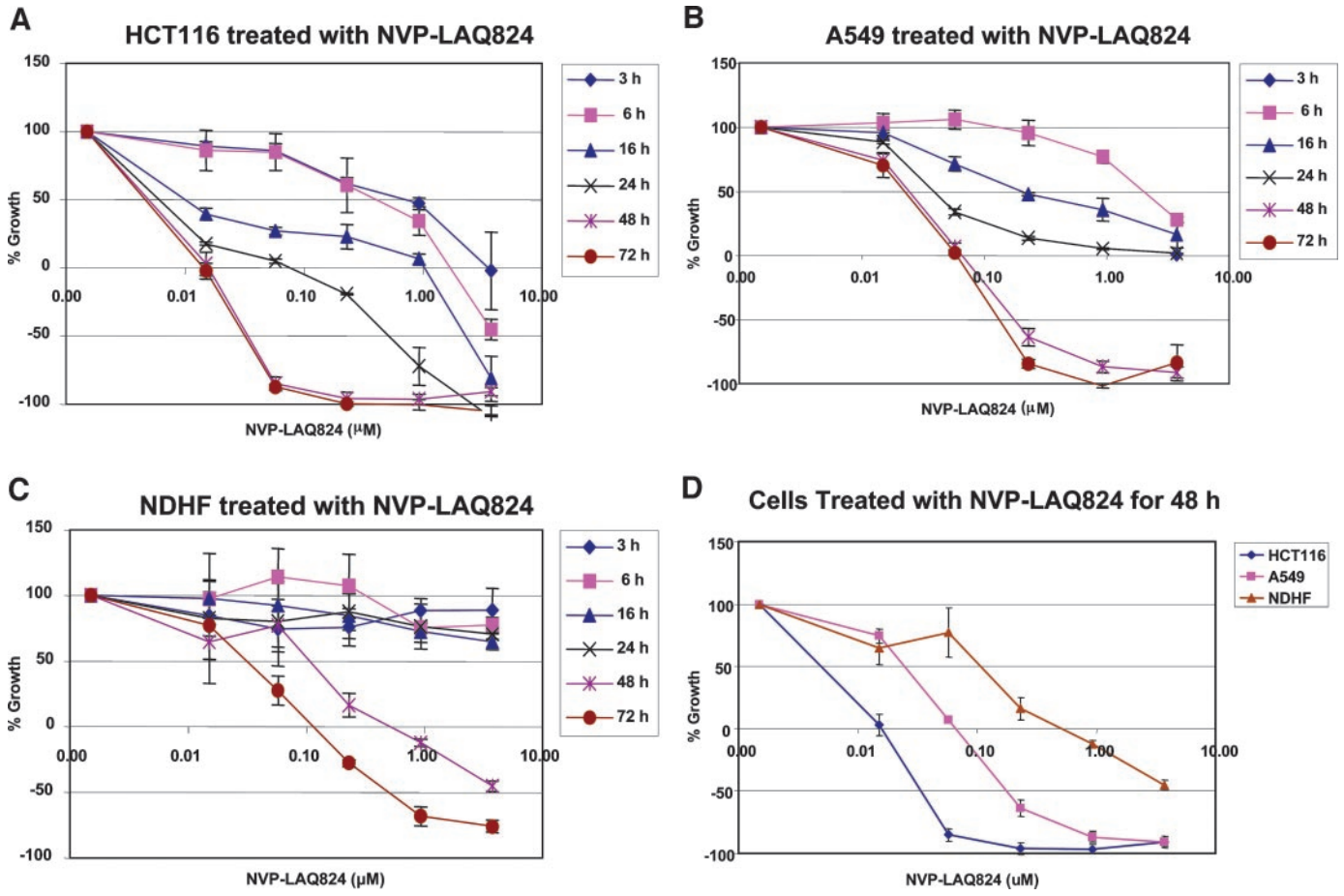

Fig. 2. Time-dependent effects of NVP-LAQ824 on cell growth and viability. The experiments were performed as described in Table 3. All experiments were conducted in triplicate and repeated at least three times. Data points are percent mean growth ± SD. *A*, treatment in HCT116 cells. *B*, treatment in A549 cells. *C*, treatment in NDHF cells. *D*, compilation of all three cell lines from 48-h exposure to NVP-LAQ824.

longer treatment of HCT116 cells with all three inhibitors triggered loss of G_2-M arrest accompanied by moderate to significant increased sub-G_1 populations (depicted by the blue-shaded areas), and this result was most profound with NVP-LAQ824 treatment (Fig. 4*B*). Furthermore, the concentration of SAHA and MS-275 required to achieve these effects were 10-fold or more than levels of NVP-LAQ824. Similar results were observed with a non-small cell lung carcinoma cell line, A549 (data not shown). These results suggested that NVP-LAQ824 may have a slightly different mechanism of action and may be more potent than the other two inhibitors. The results also suggest NVP-LAQ824 treatment breached/bypassed Rb-associated checkpoint mechanisms normally responsible for the G_1-S arrest, and all three treatments eventually breached G_2-M checkpoints in the tumor cells. Contrary to tumor cells, these checkpoint controls appear likely to remain intact in treated normal fibroblasts.

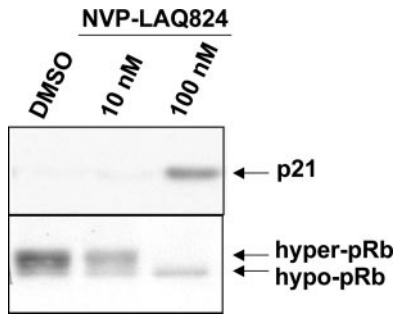

Fig. 3. NVP-LAQ824 induces p21 protein expression and Rb hypophosphorylation. A549 cells were treated with NVP-LAQ824 at the indicated concentration for 48 h. Total cell lysates were analyzed by Western blotting using antibodies for p21 (*upper panel*) and Rb (*lower panel*).

Selective Induction of Apoptosis by NVP-LAQ824 in Human Cancer Cells. The increased sub-G_1 population observed by flow cytometry in tumor cells suggested that these cells might be undergoing apoptosis. To test this hypothesis, cells were stained with Annexin V, a marker for early stages of apoptosis (green fluorescence) and propidium iodide (red fluorescence) to detect apoptotic cell death. Our data showed that a significant percentage of A549 cells (Fig. 5*A*) and the majority of HCT116 cells (Fig. 5*B*) stained positive with Annexin V after 24 h of NVP-LAQ824 exposure. By 48 h, the majority of A549 and HCT116 cells stained positive with Annexin V and/or propidium iodide, indicating that NVP-LAQ824 induced apoptotic death in these tumor cells (Fig. 5, *A* and *B*). In contrast, NDHF cells did not show noticeable Annexin V staining at the 24-h time point, and limited staining was observed after 48 h of treatment (Fig. 5*C*). A similar difference in apoptotic sensitivity to NVP-LAQ824 was observed between hTERT/SV40 T antigen transformed and untransformed human bronchial epithelial cells where Annexin V-stained cells were detected only in transformed cells (Fig. 5*D*). Thus, unlike cancer cells, normal fibroblasts most likely underwent nonlethal growth arrest upon NVP-LAQ824 treatment, as suggested by the results of cell cycle profiling and experiments staining for a marker of apoptosis. Taken together, our data indicated that NVP-LAQ824 selectively induced apoptosis in tumor cells while arresting normal cells at the G_1-S and G_2-M checkpoints.

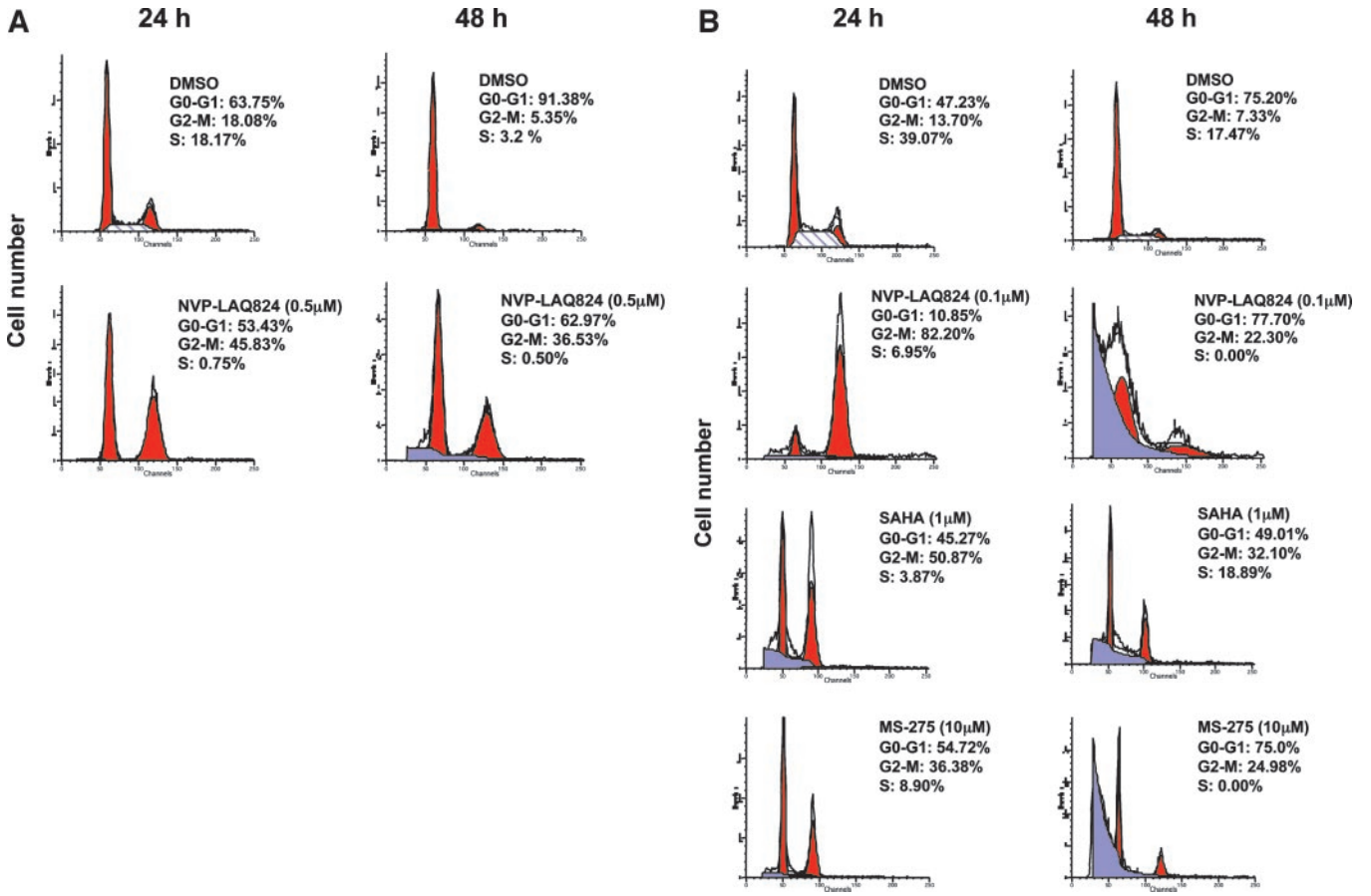

Fig. 4. Cell cycle alterations in response to NVP-LAQ824 treatment. NDHF cells were treated with NVP-LAQ824 (0.5 μM) for 24 and 48 h. In addition, HCT116 cells were treated with NVP-LAQ824 (0.1 μM), MS-275 (10 μM), and SAHA (1 μM) for 24 and 48 h. Cell cycle profiles were analyzed by flow cytometry, and the percentage of the cells in G_0-G_1, S, and G_2 phases were calculated by the ModFit program and are shown. *A*, cell cycle profiles of NDHF cells at 24 and 48 h. *B*, cell cycle profiles of HCT116 cells at 24 and 48 h.

NPV-LAQ824 Increased Acetylation of Histones H3 and H4. To confirm that the effects of NVP-LAQ824 observed in cultured cells were attributable to inhibition of HDACs, we examined the acetylation state of histones in HCT116 and A549 cells after treatment with NVP-LAQ824 (Fig. 6). Western blotting analyses using antibodies specific for acetylated histone H3 and H4 revealed a dramatic increase in the amount of histone acetylation after NVP-LAQ824 exposure for 3 h. Furthermore, the increase in acetylation reached a

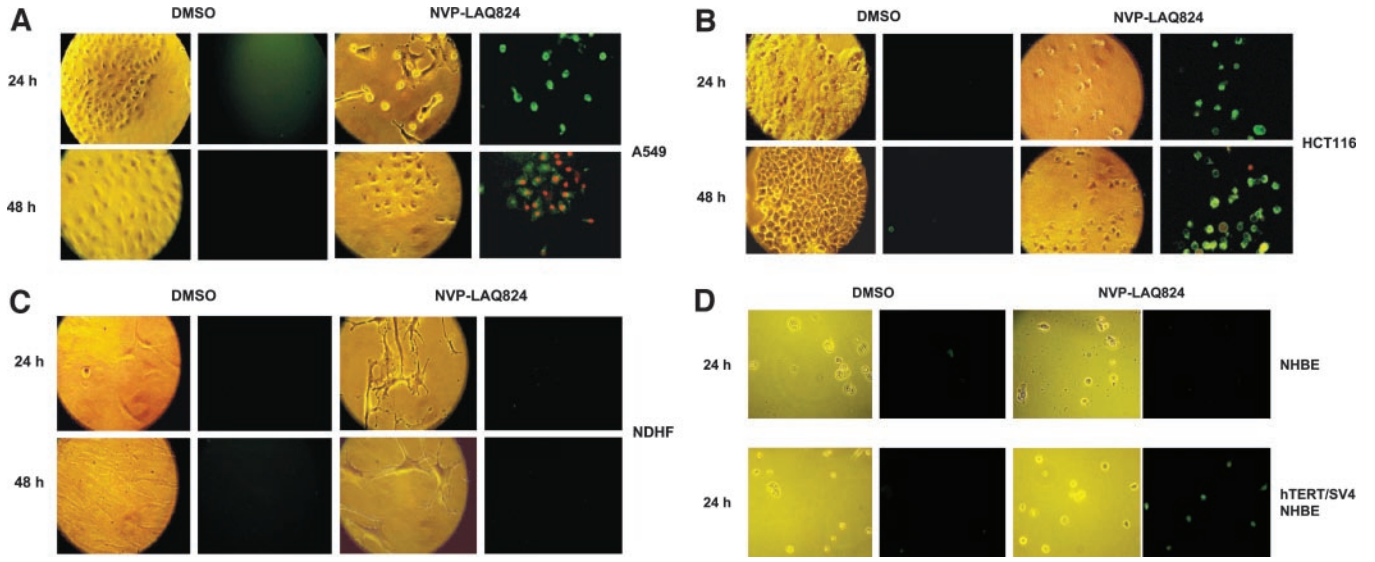

Fig. 5. Detection of apoptosis by Annexin V staining. A549 (0.5 μM), HCT116 (0.1 μM), and NDHF (0.5 μM) cells were treated with NVP-LAQ824 for 24 and 48 h. NHBE (1 μM) and hTERT/SV40 NHBE (0.1 μM) cells were treated with NVP-LAQ824 for 24 h. Cells were stained with Annexin V (*green fluorescence*) and propidium iodide (*red fluorescence*) as described in "Materials and Methods." Experiments were repeated at least two times, and representative results are shown. *A*, treatment of A549 cells. *B*, treatment of HCT116 cells. *C*, treatment of NDHF cells. *D*, treatment of NHBE and hTERT/SV40 NHBE cells.

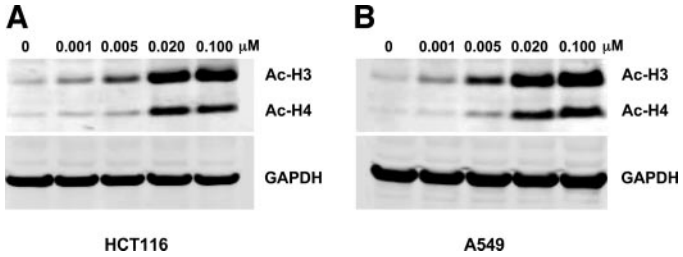

Fig. 6. NVP-LAQ824 treatment increased histone H3 and H4 acetylation in tumor cells. HCT116 and A549 cells were treated with the indicated concentrations of NVP-LAQ824 for 3 h. Acetylation levels of histones H3 (*Ac-H3*) and H4 (*Ac-H4*) were analyzed by Western blotting. The amount of GAPDH was examined to ensure equal loading of samples in each lane.

plateau at ~0.02 μM NVP-LAQ824. In contrast, the amount of GAPDH was not affected under the same experimental conditions (Fig. 6). These results suggested that NVP-LAQ824 acted as a potent HDACI in human cancer cell lines.

NVP-LAQ824 Exhibited Antitumor Activities in HCT116 Tumor Xenografts in Athymic Nude Mice. To assess the ability of NVP-LAQ824 to inhibit tumor growth, we examined its effects in s.c. implanted tumors in athymic nude mice. Tumors arose from HCT116 cells and reached an average size of 100 mm^3 before NVP-LAQ824 or vehicle was administered i.v. once daily, 5 days/week for a total of 15 doses. Tumor sizes were measured every 7 days after implantation. As shown in Fig. 7, NVP-LAQ824 treatment produced a dose-dependent inhibition of tumor growth; at 100 mg/kg, its antitumor effect was similar to that of 5-Fluorouracil, a standard anticancer agent. Importantly, no significant changes in animal body weight were observed even at the highest compound concentration, suggesting that the growth-inhibitory effect was tumor specific and that NVP-LAQ824 did not produce a general cytotoxicity in mice.

DISCUSSION

In this report, we describe the effects of a novel HDACI, NVP-LAQ824, in cultured tumor cells. NVP-LAQ824 inhibited the HDAC enzyme purified from tumor cells and activated the p21 promoter at low nanomolar concentrations. The compound also exhibited highly potent antiproliferative effects, including apoptosis in transformed cells and cell cycle arrest in normal fibroblasts.

NVP-LAQ824 treatment of tumor cell lines HCT116 and A549 and normal fibroblasts (NDHFs) generated different growth and apoptotic profiles. In HCT116, a tumor cell line, low nanomolar concentrations of NVP-LAQ824 initially induced only G_2-M arrest, but continued exposure for more than 24 h triggered progression to apoptosis. Incubation of HCT116 cells with other known inhibitors of HDACs, SAHA and MS-275, led to both G_1-S and G_2-M arrest followed by apoptosis. In contrast to NVP-LAQ824, the growth inhibition and apoptosis of HCT116 cells induced by SAHA and MS-275 were observable only when the cells were exposed to levels that were 10-fold or greater than concentrations of NVP-LAQ824 that promoted cell death. Upon several-fold higher NVP-LAQ824 exposure, NDHFs underwent a complete loss of S-phase and accumulated at the G_1-S and G_2-M boundaries, with minimal cell death. Moreover, the apoptotic study comparing the effects of NVP-LAQ824 on two normal cell types (fibroblast and epithelial) and two transformed epithelial cells support a sensitivity window between normal and malignant cells during NVP-LAQ824 treatment. After 24-h treatment with NVP-LAQ824, the transformed cells stained for a marker for apoptosis, while the normal cells remained unstained. It is interesting to note that despite p21 induction and hypophosphorylation of Rb, NVP-LAQ824 did not produce significant G_1-S arrests in transformed cells compared with G_1-S-arrested normal cells. We speculate that eventual death of tumor cells may be attributed to their inability to stably arrest. Preliminary studies from our laboratory have shown that differential cellular sensitivity toward NVP-LAQ824 and other HDACIs were associated with differential expression of mitotic checkpoint regulators (data not shown). Other reports have also implicated malfunction of G_2-M checkpoint mediator(s) in transformed cell lines as the culprit for the loss of growth arrest after HDACI treatment (40). Combining this study with other reports, a model can be drawn to explain behaviors of tumor cells *versus* normal cells to NVP-LAQ824 exposure, and the key may lie with identifying the defect(s) in both G_1-S and G_2-M checkpoint mechanisms. If these observations seen in NDHF cells represent response of other normal cell types to NVP-LAQ824, there might be a favorable therapeutic index between normal and tumor cells *in vivo*. Our studies in mice have shown that NVP-LAQ824 was able to inhibit tumor growth without producing general cytotoxicities in these animals.

The induction of apoptosis by NVP-LAQ824 appears to be p53 independent because cell death occurred in MDA435 (p53 mutant), HCT116, and A549 cells (both p53 wild type) but not in NDHFs (p53 wild type) cells. In addition, previous reports have shown that activation of *p21* gene expression by HDACIs was independent of the p53-binding element at the p21 promoter (20). The mechanism by which NVP-LAQ824 triggers apoptosis in tumor cells is currently unknown; however, studies have shown increased expression of CD95/Fas or tumor necrosis factor-related apoptosis-inducing ligand, key components of the apoptotic pathways, in response to HDACI (41, 42).

The growth-inhibitory effects of NVP-LAQ824 were time dependent and required at least 16 h to produce lethality in tumor cells. Removal of the compound in <16 h rescued cells from death. These findings suggest that NVP-LAQ824-induced cell killing is a con-

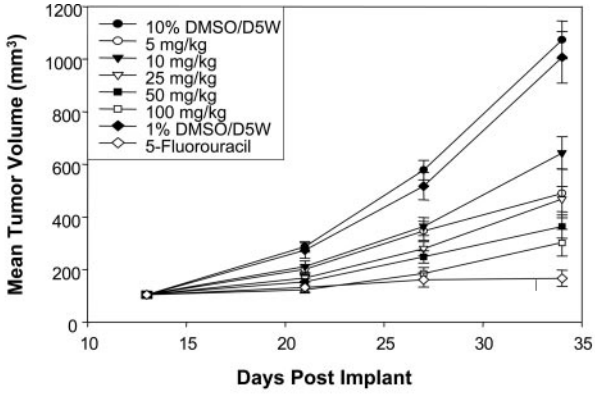

Compound	Dose (mg/kg)	% T/C	Body Weight Change (%)
NVP-LAQ824	5	40	3.2 ± 0.31
NVP-LAQ824	10	55	2.7 ± 0.50
NVP-LAQ824	25	38	0.0 ± 0.49
NVP-LAQ824	50	27	2.3 ± .33
NVP-LAQ824	100	20	1.4 ± 0.33
5-Fluorouracil	100	7	2.3±1.07

Fig. 7. Antitumor activity of NVP-LAQ824 in tumor xenografts in nude mice. Growth curves of HCT116 and human colon tumor xenografts are shown and expressed as mean tumor volume ± SE. The mice were treated with NVP-LAQ824 dissolved in the delivery vehicle (5% dextrose in water) or 5-Fluorouracil (in 10% DMSO/D5W) at the indicated concentrations. *T/C* represents the ratio of compound-treated tumor volume to vehicle-treated tumor volume, expressed as a percentage. The reduction of tumor volume between all compound-treated *versus* vehicle-treated animals showed statistical significance $P < 0.05$.

trolled specific event that probably requires changes in gene expression before an irreversible trigger forces tumor cells to their fates. This hypothesis is consistent with the mechanism of action for inhibitors of HDACs that are likely to mediate their effects through alterations in the transcriptional regulatory processes. Furthermore, the ability to detect changes in the acetylation state of histones may serve as a biomarker to examine clinical samples. In conclusion, the novel HDACI, NVP-LAQ824, offers the potential to be a highly potent anticancer therapeutic.

REFERENCES

1. Struhl, K. Histone acetylation and transcriptional regulatory mechanisms. Genes Dev., *12:* 599–606, 1998.
2. Corn, P. G., Kuerbitz, S. J., van Noesel, M. M., Esteller, M., Compitello, N., Baylin, S. B., and Herman, J. G. Transcriptional silencing of the *p73* gene in acute lymphoblastic leukemia and Burkitt's lymphoma is associated with 5′ CpG island methylation. Cancer Res., *59:* 3352–3356, 1999.
3. Domann, F. E., Rice, J. C., Hendrix, M. J., and Futscher, B. W. Epigenetic silencing of *maspin* gene expression in human breast cancers. Int. J. Cancer, *85:* 805–810, 2000.
4. Schagdarsurengin, U., Gimm, O., Hoang-Vu, C., Dralle, H., Pfeifer, G. P., and Dammann, R. Frequent epigenetic silencing of the CpG island promoter of RASSF1A in thyroid carcinoma. Cancer Res., *62:* 3698–3701, 2002.
5. van Engeland, M., Roemen, G. M., Brink, M., Pachen, M. M., Weijenberg, M. P., de Bruine, A. P., Arends, J. W., van den Brandt, P. A., de Goeij, A. F., and Herman, J. G. K-ras mutations and RASSF1A promoter methylation in colorectal cancer. Oncogene, *21:* 3792–3795, 2002.
6. Gasco, M., Sullivan, A., Repellin, C., Brooks, L., Farrell, P. J., Tidy, J. A., Dunne, B., Gusterson, B., Evans, D. J., and Crook, T. Coincident inactivation of 14-3-3σ and p16INK4a is an early event in vulval squamous neoplasia. Oncogene, *21:* 1876–1881, 2002.
7. Sharpless, N. E., Bardeesy, N., Lee, K. H., Carrasco, D., Castrillon, D. H., Aguirre, A. J., Wu, E. A., Horner, J. W., and DePinho, R. A. Loss of p16Ink4a with retention of p19Arf predisposes mice to tumorigenesis. Nature (Lond.), *413:* 86–91, 2001.
8. Yanagawa, N., Tamura, G., Oizumi, H., Takahashi, N., Shimazaki, Y., and Motoyama, T. Frequent epigenetic silencing of the *p16* gene in non-small cell lung cancers of tobacco smokers. Jpn. J. Cancer Res., *93:* 1107–1113, 2002.
9. Boivin, A. J., Momparler, L. F., Hurtubise, A., and Momparler, R. L. Antineoplastic action of 5-aza-2′-deoxycytidine and phenylbutyrate on human lung carcinoma cells. Anticancer Drugs, *13:* 869–874, 2002.
10. Shinagawa, T., Nomura, T., Colmenares, C., Ohira, M., Nakagawara, A., and Ishii, S. Increased susceptibility to tumorigenesis of ski-deficient heterozygous mice. Oncogene, *20:* 8100–8108, 2001.
11. Won, J., Yim, J., and Kim, T. K. Sp1 and Sp3 recruit histone deacetylase to repress transcription of human telomerase reverse transcriptase (hTERT) promoter in normal human somatic cells. J. Biol. Chem., *277:* 38230–38238, 2002.
12. Han, J. W., Ahn, S. H., Park, S. H., Wang, S. Y., Bae, G. U., Seo, D. W., Kwon, H. K., Hong, S., Lee, H. Y., Lee, Y. W., and Lee, H. W. Apicidin, a histone deacetylase inhibitor, inhibits proliferation of tumor cells via induction of p21WAF1/Cip1 and gelsolin. Cancer Res., *60:* 6068–6074, 2000.
13. Marks, P. A., Richon, V. M., and Rifkind, R. A. Histone deacetylase inhibitors: inducers of differentiation or apoptosis of transformed cells. J. Natl. Cancer Inst., *92:* 1210–1216, 2000.
14. Greenberg, V. L., Williams, J. M., Cogswell, J. P., Mendenhall, M., and Zimmer, S. G. Histone deacetylase inhibitors promote apoptosis and differential cell cycle arrest in anaplastic thyroid cancer cells. Thyroid, *11:* 315–325, 2001.
15. Jaboin, J., Wild, J., Hamidi, H., Khanna, C., Kim, C. J., Robey, R., Bates, S. E., and Thiele, C. J. MS-27–275, an inhibitor of histone deacetylase, has marked *in vitro* and *in vivo* antitumor activity against pediatric solid tumors. Cancer Res., *62:* 6108–6115, 2002.
16. Furumai, R., Komatsu, Y., Nishino, N., Khochbin, S., Yoshida, M., and Horinouchi, S. Potent histone deacetylase inhibitors built from trichostatin A and cyclic tetrapeptide antibiotics including trapoxin. Proc. Natl. Acad. Sci. USA, *98:* 87–92, 2001.
17. Fournel, M., Trachy-Bourget, M. C., Yan, P. T., Kalita, A., Bonfils, C., Beaulieu, C., Frechette, S., Leit, S., Abou-Khalil, E., Woo, S. H., Delorme, D., MacLeod, A. R., Besterman, J. M., and Li, Z. Sulfonamide anilides, a novel class of histone deacetylase inhibitors, are antiproliferative against human tumors. Cancer Res., *62:* 4325–4330, 2002.
18. Kim, Y. B., Ki, S. W., Yoshida, M., and Horinouchi, S. Mechanism of cell cycle arrest caused by histone deacetylase inhibitors in human carcinoma cells. J. Antibiot. (Tokyo), *53:* 1191–1200, 2000.
19. Richon, V. M., Zhou, X., Rifkind, R. A., and Marks, P. A. Histone deacetylase inhibitors: development of suberoylanilide hydroxamic acid (SAHA) for the treatment of cancers. Blood Cells Mol. Dis., *27:* 260–264, 2001.
20. Sambucetti, L. C., Fischer, D. D., Zabludoff, S., Kwon, P. O., Chamberlin, H., Trogani, N., Xu, H., and Cohen, D. Histone deacetylase inhibition selectively alters the activity and expression of cell cycle proteins leading to specific chromatin acetylation and antiproliferative effects. J. Biol. Chem., *274:* 34940–34947, 1999.
21. Strait, K. A., Dabbas, B., Hammond, E. H., Warnick, C. T., Iistrup, S. J., and Ford, C. D. Cell cycle blockade and differentiation of ovarian cancer cells by the histone deacetylase inhibitor trichostatin A are associated with changes in p21, Rb, and Id proteins. Mol. Cancer Ther., *1:* 1181–1190, 2002.
22. Slack, J. L. The biology and treatment of acute progranulocytic leukemia. Curr. Opin. Oncol., *11:* 9–13, 1999.
23. Amann, J. M., Nip, J., Strom, D. K., Lutterbach, B., Harada, H., Lenny, N., Downing, J. R., Meyers, S., and Hiebert, S. W. ETO, a target of t(8;21) in acute leukemia, makes distinct contacts with multiple histone deacetylases and binds mSin3A through its oligomerization domain. Mol. Cell. Biol., *21:* 6470–6483, 2001.
24. Gelmetti, V., Zhang, J., Fanelli, M., Minucci, S., Pelicci, P. G., and Lazar, M. A. Aberrant recruitment of the nuclear receptor corepressor-histone deacetylase complex by the acute myeloid leukemia fusion partner ETO. Mol. Cell. Biol., *18:* 7185–7191, 1998.
25. Ferrara, F. F., Fazi, F., Bianchini, A., Padula, F., Gelmetti, V., Minucci, S., Mancini, M., Pelicci, P. G., Lo, C. F., and Nervi, C. Histone deacetylase-targeted treatment restores retinoic acid signaling and differentiation in acute myeloid leukemia. Cancer Res., *61:* 2–7, 2001.
26. Petti, M. C., Fazi, F., Gentile, M., Diverio, D., De Fabritiis, P., De Propris, M. S., Fiorini, R., Spiriti, M. A., Padula, F., Pelicci, P. G., Nervi, C., and Lo, C. F. Complete remission through blast cell differentiation in PLZF/RARα-positive acute promyelocytic leukemia: *in vitro* and *in vivo* studies. Blood, *100:* 1065–1067, 2002.
27. Saito, A., Yamashita, T., Mariko, Y., Nosaka, Y., Tsuchiya, K., Ando, T., Suzuki, T., Tsuruo, T., and Nakanishi, O. A synthetic inhibitor of histone deacetylase, MS-27-275, with marked *in vivo* antitumor activity against human tumors. Proc. Natl. Acad. Sci. USA, *96:* 4592–4597, 1999.
28. Lavelle, D., Chen, Y. H., Hankewych, M., and DeSimone, J. Histone deacetylase inhibitors increase p21(WAF1) and induce apoptosis of human myeloma cell lines independent of decreased IL-6 receptor expression. Am. J. Hematol., *68*: 170–178, 2001.
29. Suzuki, T., Yokozaki, H., Kuniyasu, H., Hayashi, K., Naka, K., Ono, S., Ishikawa, T., Tahara, E., and Yasui, W. Effect of trichostatin A on cell growth and expression of cell cycle- and apoptosis-related molecules in human gastric and oral carcinoma cell lines. Int. J. Cancer, *88:* 992–997, 2000.
30. Richon, V. M., Webb, Y., Merger, R., Sheppard, T., Jursic, B., Ngo, L., Civoli, F., Breslow, R., Rifkind, R. A., and Marks, P. A. Second generation hybrid polar compounds are potent inducers of transformed cell differentiation. Proc. Natl. Acad. Sci. USA, *93(12):* 5705–5708, 1996.
31. Pina, I. C., Gautschi, J. T., Wang, G. Y., Sanders, M. L., Schmitz, F. J., France, D., Cornell-Kennon, S., Sambucetti, L. C., Remiszewski, S. W., Perez, L. B., Bair, K. W., and Crews, P. Psammaplins from the sponge *Pseudoceratina purpurea*: inhibition of both histone deacetylase and DNA methyltransferase. J. Org. Chem., *68(10):* 3866–3873, 2003.
32. Remiszewski, S. W. The discovery of NVP-LAQ824: from concept to clinic. Curr. Med. Chem., *10(22):* 2393–402, 2003.
33. Yoshida, M., Furumai, R., Nishiyama, M., Komatsu, Y., Nishino, N., and Horinouchi, S. Histone deacetylase as a new target for cancer chemotherapy. Cancer Chemother. Pharmacol., *48 Suppl 1:* S20–S26, 2001.
34. Marks, P., Rifkind, R. A., Richon, V. M., Breslow, R., Miller, T., and Kelly, W. K. Histone deacetylases and cancer: causes and therapies. Nat. Rev. Cancer *1:* 194–202, 2001.
35. Pelicci, P. G. A new class of anti-cancer drugs: HDAC-inhibitors. Suppl. Tumori, *1:* S66, 2002.
36. Vigushin, D. M., and Coombes, R. C. Histone deacetylase inhibitors in cancer treatment. Anticancer Drugs, *13:* 1–13, 2002.
37. Sowa, Y., Orita, T., Minamikawa, S., Nakano, K., Mizuno, T., Nomura, H., and Sakai, T. Histone deacetylase inhibitor activates the WAF1/Cip1 gene promoter through the Sp1 sites. Biochem. Biophys. Res. Commun., *241:* 142–150, 1997.
38. Qiu, L., Burgess, A., Fairlie, D. P., Leonard, H., Parsons, P. G., and Gabrielli, B. G. Histone deacetylase inhibitors trigger a G2 checkpoint in normal cells that is defective in tumor cells. Mol. Biol. Cell, *11:* 2069–2083, 2000.
39. Glick, R. D., Swendeman, S. L., Coffey, D. C., Rifkind, R. A., Marks, P. A., Richon, V. M., and La Quaglia, M. P. Hybrid polar histone deacetylase inhibitor induces apoptosis and CD95/CD95 ligand expression in human neuroblastoma. Cancer Res., *59:* 4392–4399, 1999.
40. Inoue, H., Shiraki, K., Ohmori, S., Sakai, T., Deguchi, M., Yamanaka, T., Okano, H., and Nakano, T. Histone deacetylase inhibitors sensitize human colonic adenocarcinoma cell lines to TNF-related apoptosis inducing ligand-mediated apoptosis. Int. J. Mol. Med., *9:* 521–525, 2002.
41. Suzuki, T., Ando, T., Tsuchiya, K., Fukazawa, N., Saito, A., Mariko, Y., Yamashita, T., and Nakanishi, O. Synthesis and histone deacetylase inhibitory activity of new benzamide derivatives. J. Med. Chem., *42(15):* 3001–3003, 1999.